Journal of Luminescence 203 (2018) 371–375

Contents lists available at ScienceDirect

Journal of Luminescence

journal homepage: www.elsevier.com/locate/jlumin

Synthesis and photoluminescence properties of deep red-emitting $CaGdAlO_4$:Mn^{4+} phosphors for plant growth LEDs

Qi Sun, Shaoying Wang, Bin Li, Heng Guo, Xiaoyong Huang*

Key Lab of Advanced Transducers and Intelligent Control System, Ministry of Education and Shanxi Province, College of Physics and Optoelectronics, Taiyuan University of Technology, Taiyuan 030024, PR China

ARTICLE INFO

Keywords:
Phosphors
Photoluminescence
Red emissions
$CaGdAlO_4$
Mn^{4+} ions
Deep-red LED

ABSTRACT

In this work, we reported on novel Mn^{4+}-activated $CaGdAlO_4$ (CGA) deep red-emitting phosphors. Under 349 nm excitation, the CGA:Mn^{4+} phosphors showed a deep-red emission band within the wavelength range of 650–800 nm centered at 715 nm due to the $^2E_g \rightarrow {}^4A_{2g}$ transition of Mn^{4+} ions. CGA:Mn^{4+} phosphors had two broad excitation bands in the 250–550 nm region. The optimal doping concentration of Mn^{4+} was about 0.2 mol%. The CIE chromaticity coordinates of CGA:0.2%Mn^{4+} sample were (0.7132, 0.2866), and the lifetimes of CGA:$x$$Mn^{4+}$ phosphors monitored at 715 nm showed a decrease with increasing Mn^{4+} doping concentration in the range of 0.05–1.0 mol%. Importantly, the CGA:0.2%Mn^{4+} sample had internal quantum efficiency as high as 45%. Finally, a deep-red LED device was prepared by integrating a 365 nm near-UV InGaN chip and CGA:0.2% Mn^{4+} phosphors.

1. Introduction

Nowadays, with the rapid development of society, energy saving attracts extensive attention and becomes a significant matter [1–5]. Therefore, white light-emitting diodes (WLEDs) have become promising candidates to replace conventional light sources such as fluorescent and incandescent lamps due to their superior advantages such as high efficiencies, long lifetimes, low energy consumption and environment friendliness [6–12]. Given these advantages, WLEDs are widely used in various application areas. Recently, light-emitting diodes (LEDs) have been recognized as the light sources for plant growth and have been widely applied in indoor plant cultivation. It has been reported that blue light around 450 nm (410–500 nm) affects photosynthesis, red light around 660 nm (610–700 nm) may be helpful for phototropism, and far-red light around 730 nm (700–740 nm) promotes photomorphogenesis [13].

Mn^{4+} ion with a $3d^3$ electron configuration can show deep red emission due to $^2E_g \rightarrow {}^4A_{2g}$ transitions of Mn^{4+}. In addition, Mn^{4+} ions can be stable when Mn^{4+} ions occupy octahedral or distorted octahedral environment by substituting Ti^{4+}, W^{6+}, Al^{3+}, and Ge^{4+} ions [14–17]. Therefore, Mn^{4+} doped oxide-based phosphors are expected to be non-rare-earth red phosphors for indoor plant cultivation [18]. Recently, Mn^{4+}-activated oxide-based red phosphors have been extensively studied [19]. In this paper, we reported Mn^{4+}-activated $CaGdAlO_4$ (CGA) deep red-emitting phosphors. Upon 349 nm excitation, an intense deep-red emission with a maximum peak centered at 715 nm was observed. The optimal Mn^{4+} ions doping concentration was about 0.2 mol%. The CIE chromaticity coordinates of CGA:0.2%Mn^{4+} sample were (0.7132, 0.2866), and moreover, the CGA:0.2%Mn^{4+} sample had internal quantum efficiency (IQE) of 45% when excited at 349 nm. More importantly, the emission band of CGA:Mn^{4+} phosphors was well-matched with the absorption band of phytochrome P_{FR}. All the results suggested that the CGA:Mn^{4+} phosphors could be promising deep red-emitting phosphor candidates for application in the red LEDs for indoor plant cultivation.

2. Experimental

A series of CGA:$x$$Mn^{4+}$ (x = 0.05, 0.1, 0.2, 0.4, 0.6, 0.8, and 1.0 mol %) phosphors were prepared through a high-temperature solid-state reaction route. $CaCO_3$ (analytical reagent, AR), Gd_2O_3 (99.99%), Al_2O_3 (AR), and $MnCO_3$ (AR) were used as the raw materials. According to the stoichiometric ratio, these raw materials were weighed and ground in an agate mortar. Then, the obtained mixtures were transferred to the heating furnace and pre-calcined at 500 °C for 3 h, then calcined again at 1500 °C for 5 h. The final products were ground again for further characterization. The X-ray diffraction (XRD) patterns of the samples were recorded on a Bruker D8 X-ray diffractometer using Cu Kα radiation. The photoluminescence (PL) and PL excitation (PLE) spectra and decay curves were measured by an Edinburgh FS5 spectrometer

---

* Corresponding author.
E-mail address: huangxy04@126.com (X. Huang).

https://doi.org/10.1016/j.jlumin.2018.06.072
Received 9 May 2018; Received in revised form 9 June 2018; Accepted 25 June 2018
Available online 26 June 2018
0022-2313/ © 2018 Elsevier B.V. All rights reserved.

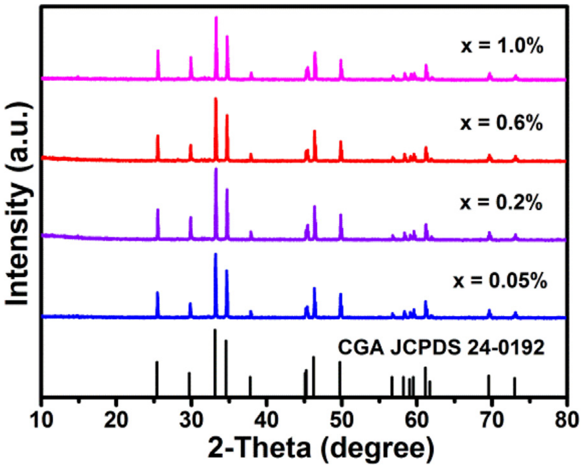

Fig. 1. XRD patterns of CGA:xMn^{4+} (x = 0.05%, 0.2%, 0.6% and 1.0%) phosphors. The standard data of CGA (JCPDS no. 24–0192) were also shown as references.

equipped with a 150 W continued-wavelength Xenon lamp and a pulsed Xenon lamp, respectively. The IQE was measured by an Edinburgh FS5 spectrometer equipped with an integrating sphere coated with $BaSO_4$.

3. Results and discussion

Fig. 1 shows the XRD patterns of CGA:xMn^{4+} (x = 0.05%, 0.2%, 0.6%, and 1.0%) samples. It can be seen that all of the diffraction peaks of the samples were matched well with the standard card of CGA (JCPDS no. 24-0192). No other crystalline phases were observed after Mn^{4+} ions were added. It can be said that Mn^{4+} ions were well-doped into the host with no significant influence on the structure of CGA. The CGA has tetragonal K_2NiF_4 structure with the space group I4/mmm ($D_{17}{}^{4h}$) [20]. Moreover, the Ca^{2+} and Gd^{3+} ions occupy nine-coordination sites and Al^{3+} occupies the six-coordinate site forming an octahedron. Considering the ionic radii of Ca^{2+} (r = 1.18 Å, CN = 9), Gd^{3+} (r = 0.938 Å, CN = 9), Al^{3+} (r = 0.535 Å, CN = 6), and Mn^{4+} (r = 0.53 Å, CN = 6) ions [20], it is obvious that Mn^{4+} preferred to occupy Al^{3+} site in the CGA host.

Fig. 2(a) presents the PLE and PL spectra of CGA:0.2%Mn^{4+} sample. When monitored at 715 nm, the PLE spectrum showed two broad bands within the range from 250 nm to 550 nm, which can be well-fitted with Gaussian functions into four bands centered at 298 nm, 352 nm, 394 nm and 489 nm, respectively. These bands assigned to the Mn-O charge transfer band (CTB), and the Mn^{4+} spin-allowed transitions of $^4A_2 \rightarrow {}^4T_1$, $^4A_2 \rightarrow {}^2T_2$, $^4A_2 \rightarrow {}^4T_2$, respectively [14]. The sharp lines in the range of 450–500 nm were due to the background during the measurement. Under 349 nm excitation, there was one narrow emission band between 650 nm and 800 nm with a sharp peak at 715 nm, which was due to the spin-forbidden $^2E_g \rightarrow {}^4A_{2g}$ transition of Mn^{4+} [21]. Fig. 2(b) shows the PL spectrum of CGA:0.2%Mn^{4+} phosphors and the absorption spectra of phytochrome P_{FR}. It can be seen that there is a significant overlap between the emission band of CGA:0.2%Mn^{4+} phosphors and the absorption of phytochrome P_{FR}. Thus, the CGA:Mn^{4+} phosphors could be promising deep red-emitting phosphor candidates for indoor plant cultivation.

Fig. 3(a) shows the PL spectra of CGA:xMn^{4+} (x = 0.05%, 0.1%, 0.2%, 0.4%, 0.6%, 0.8% and 1.0%) phosphors under 349 nm excitation. All of the spectra were similar to each other except for the emission intensity. It can be seen that with an increase of x from 0.05% to 1.0%, the emission intensity increased until it reached a maximum at x = 0.2%, whereas further increasing Mn^{4+} ions concentration resulted in declined emission intensity due to the concentration quenching effect. Herein, the critical distance (R_c) between Mn^{4+} ions can be roughly evaluated using the following equation [22]:

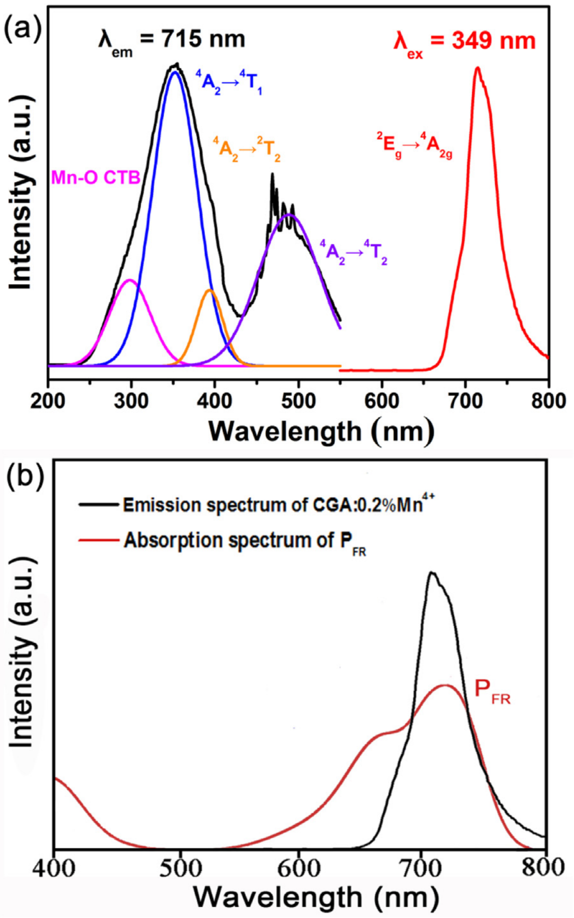

Fig. 2. (a) PLE and PL spectra of CGA:0.2%Mn^{4+} sample. (b) PL spectrum of CGA:0.2%Mn^{4+} phosphors and the absorption spectra of phytochrome P_{FR}.

$$R_c \approx 2\left[\frac{3V}{4\pi X_c N}\right]^{1/3}, \tag{1}$$

here R_c is the critical distance, V is the volume of the host lattice, X_c refers to the critical doping concentration of Mn^{4+}, and N is the number of available sites for the dopant in the unit cell. In this work, the X_c = 0.2%; V = 160.82 Å^3; N = 2, respectively [20]. Therefore, the calculated R_c value for Mn^{4+} was 42.50 Å, which was larger than 5 Å. The possibility of exchange interaction among Mn^{4+} ions in the CGA host may be excluded because the R_c of exchange interaction is normally less than 5 Å. Therefore it can be deduced that the energy transfer mechanism among Mn^{4+} ions was the electric multipolar interaction. The type of interaction mechanism between Mn^{4+} ions can be calculated by the following equation [23]:

$$\log(I/x) = \text{A} - (\theta/3)\log x, \tag{2}$$

where I is the emission intensity, x is the dopant concentration, A is concentration, and θ = 6, 8 and 10 corresponds to dipole-dipole, dipole-quadrupole and quadrupole-quadrupole interactions, respectively. Fig. 3(b) shows the relationship between log(I/x) and log(x), which was well linearly fitted with a slope (-θ/3) = −1.216. Thus θ = 3.648, which was close to 3, suggesting that the concentration quenching mechanism of CGA:Mn^{4+} was the non-radiative energy transfer among the nearest-neighbor ions [24].

Fig. 4 shows the decay curves of CGA:xMn^{4+} samples monitored at 715 nm under the excitation of 349 nm. All the decay curves could be well-fitted with a single-exponential function as follows equation [25]:

$$I_t = I_0 exp(-t/\tau) + A \tag{3}$$

in which I_t is the luminescence intensity at time t, I_0 is the initial

Download English Version:

https://daneshyari.com/en/article/7839720

Download Persian Version:

https://daneshyari.com/article/7839720

Daneshyari.com